Alfven wave studies on PRETEXT

P. M. Valanju, R. D. Bengtson, W. D. Booth, R. W. Cook, T. E. Evans, S. M. Mahajan, M. E. Oakes, D. W. Ross, and Clifford M. Surko

Citation: AIP Conference Proceedings **129**, 1 (1985); doi: 10.1063/1.35263
View online: http://dx.doi.org/10.1063/1.35263
View Table of Contents:
http://scitation.aip.org/content/aip/proceeding/aipcp/129?ver=pdfcov
Published by the AIP Publishing

Alfven Wave Studies on PRETEXT.*

P.M. Valanju, R.D. Bengtson, W.D. Booth, R.W. Cook,
T.E. Evans, S.M. Mahajan, M.E. Oakes, D.W. Ross,

The University of Texas at Austin

and

Clifford M. Surko

AT&T Bell Laboratories,
Murray Hill, New Jersey 07974

Abstract:
The properties of low frequency Alfven waves in hot, magnetically confined plasmas are quite unlike those in homogeneous media. Extensive theoretical studies have uncovered the Alfven continuum along with global Alfven eigenmodes (GAE). It has been suggested that such modes may be good candidates for rf heating below the ion cyclotron frequency. We present a unified investigation on PRETEXT of the structure of the global modes. These measurements are made using two phased toroidal antennas. The GAE are predicted to appear as resonances in the antenna loading resistance and have been observed earlier on TCA. We find that in addition to antenna resistance and inductance, signals from magnetic probes at the plasma surface also exhibit this resonant behavior. The plasma parameter dependence (i.e., the amplitude and location) of these resonances is found in good agreement with the theory. Driven plasma density fluctuations with a rich spatial structure are predicted to develop at these resonances; we have observed this structure using a CO_2 laser interferometer. Results from the laser and impedance measurements along with antenna phasing permit assignment of mode numbers. Since the two-antenna configuration can simultaneously excite more than one mode in the plasma, the resulting interference effects demand careful interpretation of the spatial and temporal mode structures seen. These interference effects provide both a challenge and an opportunity for an optimum antenna design in an Alfven heating experiment.

The properties of low frequency Alfven waves in hot, magnetically confined plasma are quite unlike those in homogeneous media. Theoretical studies have uncovered the Alfven continuum along with global Alfven eigenmodes (GAE). It has been suggested that such modes may be good candidates for rf heating below the ion cyclotron frequency. In this talk, we present the results of a joint theoretical and experimental investigation of the spatial properties and dispersion relations of the GAE. These experiments were conducted on the PRETEXT tokamak at the University of Texas at Austin (Ref. 1). The tokamak parameters are summarized in Table 1. The frequency region of interest for these parameters is below 10 MHz. To drive the rf currents, we use either a 100 kw tuned amplifier at 2.1 MHz or a 1 kw broadband amplifier (0.3 to 30 MHz).

0094-243X/85/1290001-7$3.00 Copyright 1985 American Institute of Physics

Table 1. Tokamak Parameters.

PRETEXT	
Major Radius = 53.3 cm	N_e = 7-27x10^{12}cm^{-3}
Minor Radius = 17.4 cm	T_e ~ 200 eV
Limiter Radius = 14 cm	B_{tor} = 8 kG
I_{plasma} = 20-35 kA	Pulse Length ~50 ms
q_{edge} ~ 6	
RF	
Amplifier Power≤100 kW	Pulse Length~50 ms
Frequency = 2.1 MHz	Capacitive Matching Circuit
Antenna-Plasma Distance = 1.5 cm	
Antenna-Wall Distance = 1.9 cm	
Antennas Connected in Parallel	
Two Toroidal Antennas (Fig. 1) with Insulating Coatings	
Impedance Measurement: Current Amplitudes and Phases	
RF Magnetic Probes: B_r and B_θ at Limiter	

The antennas consist of two 90^o toroidal segments, each 10 cm wide, made from stainless steel and coated with ceramic insulation (Fig. 1). We do not use any Faraday shields. The antennas are 1.5 cm from the plasma and 1.9 cm from the wall. They are driven in parallel by using the capacitive matching circuit shown in Fig. 2. This circuit has dual purposes; it matches the antenna impedance to the 50Ω transmission line coming from the transmitter and it also balances the currents in the two antennas to provide for the small differences in their inductances. If the two antennas and the series legs of the matching circuit are viewed as a wheatstone bridge, we have to adjust C_1 and C_2 so that there is no voltage between points a and b in Fig. 2. If this adjustment is not performed, the antenna loading with plasma becomes extremely large. Once the balancing is done, the two antenna legs of the circuit can be reduced to a single equivalent RLC circuit. We measure magnitudes of the currents I_p, I_T and I_A at the triple point O in Fig. 2. We also measure their relative phases. This allows us to calculate the effective antenna inductance L_{TOT} and resistance R_{TOT} in two independent ways. This gives a self-consistency check for the model used for the actual circuit and avoids any spurious errors. With this setup, we can measure R_{TOT} and L_{TOT} to 10% accuracy in their absolute values. Sharp peaks in R_{TOT} can be measured to an even better accuracy. The resistance R_{TOT} in vacuum is about 300mΩ, and it goes up by about 300mΩ in the presence of any plasma. This loading we call ***"background loading"***. The balancing of antennas reduces the background loading of two antennas to a level below that for a single antenna.

A typical shot is shown in Fig. 3. As the plasma current, density and toroidal field change, the predicted locations of the resonances also change. At certain values of plasma parameters we observe sharp peaks in loading resistance above the background value.

In order to compare with theory, we need to calculate the frequency and the width of a resonance from the measured plasma parameters at each time. We decompose the fluctuating electric field driven by the antenna into Fourier components as

$$E(r,t) = \sum_{l,m} E_{l,m} \exp[i(m\vartheta - l\zeta - \omega t)] \quad (1)$$

where l and m are the toroidal and poloidal mode numbers. In order to find the eigenmodes, it is necessary to solve a fourth order differential equation with the given boundary conditions. It was shown in Ref. 2 that this can be done using a variational technique. The predicted eigenfrequency for an (l,m) mode is

$$\omega^2_{lm} = \frac{(1 - \varepsilon r_0^2/m^2L^2)}{1 + (1 - \varepsilon r_0^2/m^2L^2)(\omega_{A0}/\omega_{ci})^2} \quad (2)$$

where $\varepsilon = g - (1/4) - (g - (l/2)^{1/2})$, ω^2_{A0} = miminum of $(k_{||}^2 v_A^2)$ at $r = r_0$, L and g depend on gradients of density and q profile at r_0, and ω_{ci} is the cyclotron frequency. We assume profiles of the form

$$n(r) = n_0(1 - (r/a)^2), \quad \text{and} \quad (3)$$

$$q(r) = 1 + (q_0 - 1)(r/a)^2. \quad (4)$$

Using the measured values of n_0 and q_0, we can calculate $\omega_{l,m}$ at all times in a shot. This is shown in Fig. 4. As can be seen, we find resonance peaks when the driver frequency ω is equal to the resonant frequency ω_{lm} of the (1,-2) mode. The only ambiguity is the effective mass m_{eff} which enters through the Alfven speed v_A. Since we do not measure m_{eff}, we use it as a free parameter on one shot to get a good fit and then see if it agrees on other shots at other frequencies. Also on a given shot, if we see more than one mode, only one value of m_{eff} is seen to give a consistent identification of all peaks. This, in effect, fixes m_{eff} for us.

As the resonance frequency passes through the driver frequency, we expect the L_{TOT} and R_{TOT} to show a resonant behavior. We calculate their predicted values using a numerical kinetic code developed by Ross, Chen and Mahajan (Ref. 3). These are shown in Fig. 5, while the experimental measurements are shown in Fig. 6. The agreement convinces us that we are seeing a resonant mode of the plasma. Having located one mode, we also try to track it, i.e., we try to find it at nearby frequencies. This is shown in the paper by Booth, et al. in these proceedings. The mode always appears when the (variable) driver frequency equals the predicted resonance frequency. We have done this for frequencies between 1.7 and 2.3 MHz, for which the (1,-2) mode is within our plasma parameter ranges. The agreement with the location of the predicted mode and its proper tracking give us extra confidence in our mode identification.

The second part of the experiment consists of a CO_2 laser interferometer. It measures both the phase (with respect to the driver) and the amplitude of the chord-integrated mode-associated density fluctuations, $\int ndx$. The expected behavior near a global mode is shown in Fig. 7, while the observations are shown in Fig. 6. Again, the agreement seems quite good.

The interferometer chord can be moved from shot-to-shot to produce a radial scan of the mode. After having identified the global mode, we measure its amplitude $\int ndx$, at various chord positions and generate a radial profile shown in Fig. 8. The solid line is the theoretical prediction from the numerical code of Ref. 2. It is clear that we have observed the radial structure of the (1,-2) global mode.

The radial structure of a mode and its time evolution as the plasma parameters evolve can be complicated by the presence of nearby modes. This is shown in Fig. 9 where the (1,-2) global mode can be seen to coexist with the (1,-1) continuum mode. As the density increases, one first excites a global mode which then bifurcates into two continuum (local) modes (one each near the intersection of ω with $k_{||}v_A$ in Fig. 9). The inner local mode eventually disappears. If one watched the time evolution of this process at a fixed chord, the picture one gets is very dependent on the chord chosen. For example, the maximum $\int ndx$ may not correspond to the location of the GAE if the chord is not at the radial maximum of $\int ndx$. This is seen in Fig. 9. The maximum of R_{TOT} along with the maximum slope of L_{TOT} does, however, indicate the actual occurrence of a resonant GAE. As one crosses a global mode and goes into the continuum, the interferometer signal can go through maxima both near the global mode and in the continuum. Interpretation of the $\int ndx$ data, therefore, needs extreme care.

This problem could be reduced if we had more precise mode selection. Since it is easy to phase antennas by 0°, 90° or 180°, it is logical to build the 16 antenna array (Ref. 4) shown in Fig. 10. This array will allow us to select any one of the $\pm$ l=0,1,2,3 and $\pm$m=0,1,2,3 modes, thus reducing interference between two coexistent modes. It will also allow us to choose an (l,m) mode over its counterpart (-l,-m) mode. Also, each antenna can be very small and hence easier to install. Such an antenna array is currently under construction.

*This work is supported by the Department of Energy and the Texas Atomic Energy Research Foundation.

[1] T.E. Evans, et al., *Phys. Rev. Letters* ***53***, 1743 (1984).
[2] S.M. Mahajan, *Phys. Fluids* ***27***, 2238 (1984).
[3] D.W. Ross, G.L. Chen and S.M. Mahajan, *Phys. Fluids* ***25***, 652 (1982).
[4] Internal Communications-S.M. Mahajan and P.M. Valanju.

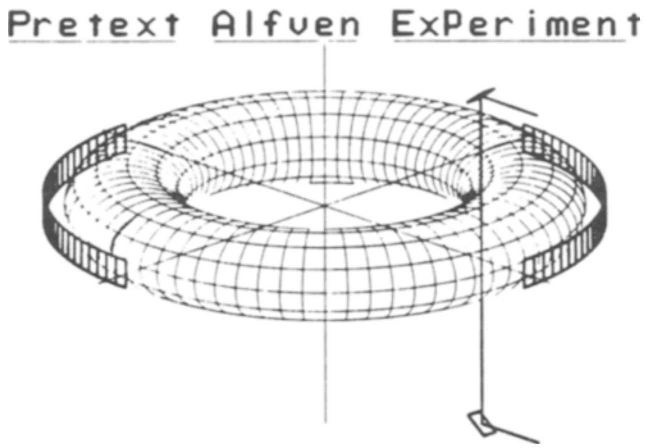

Figure 1.

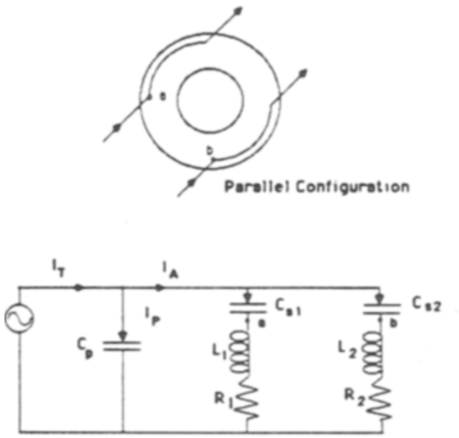

Figure 2.

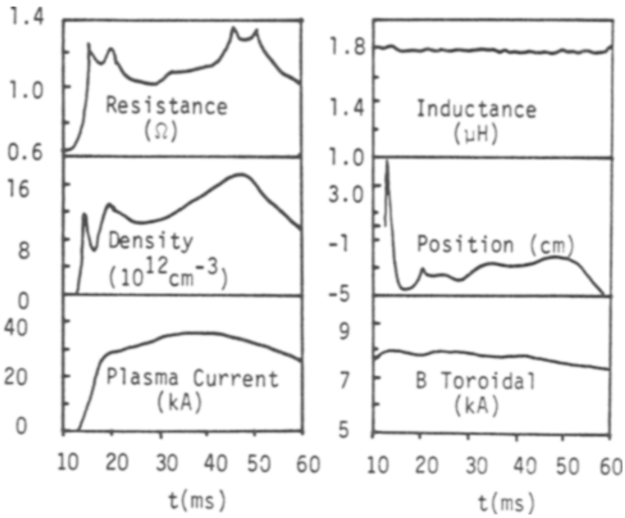

Figure 3.

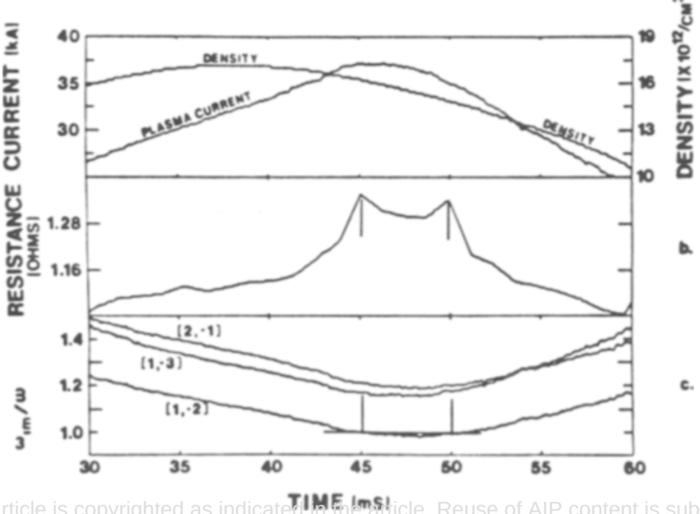

Figure 4.

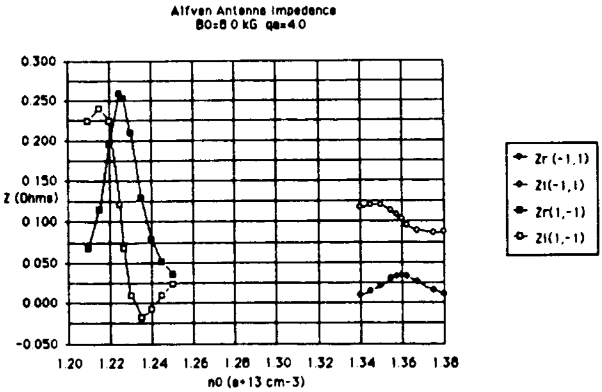

Figure 5.

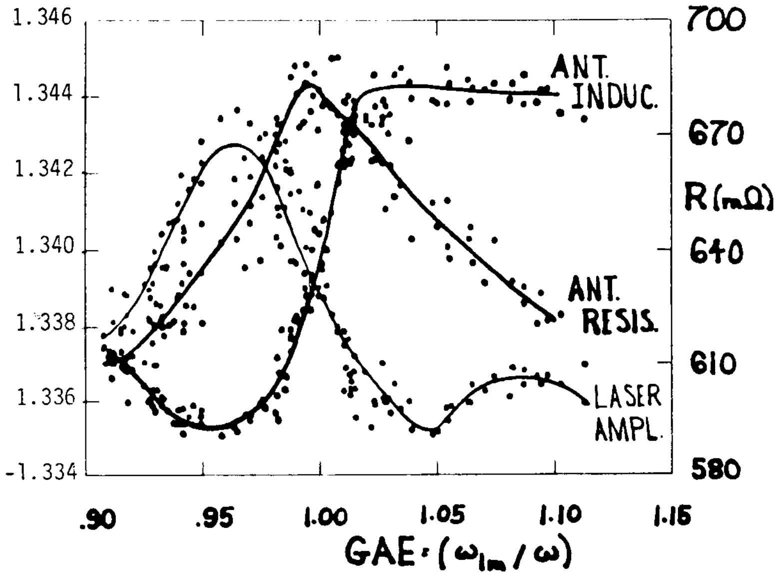

Figure 6.

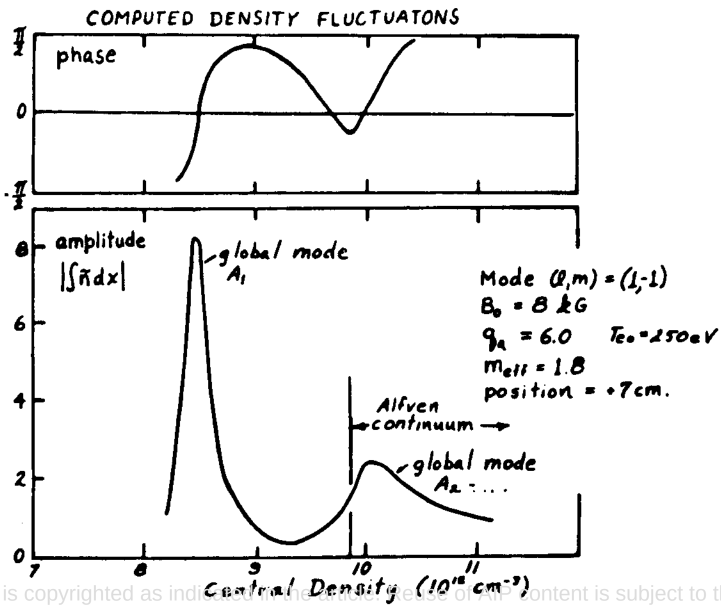

Figure 7.

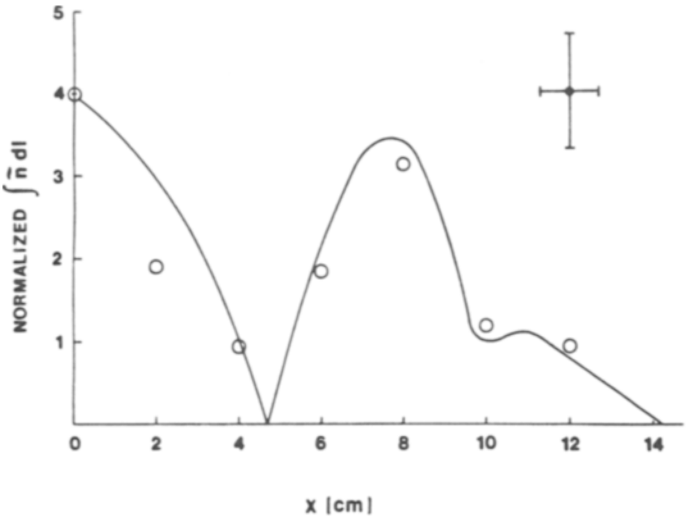

Figure 8.

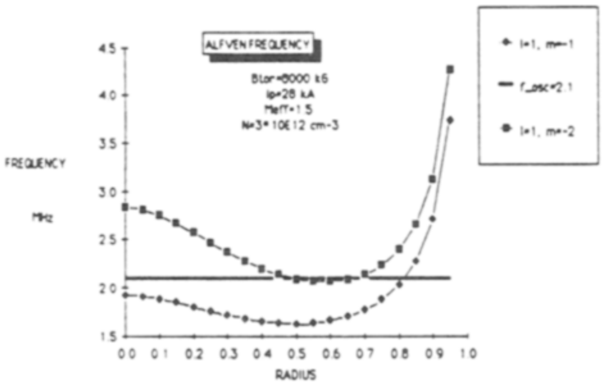

Figure 9.

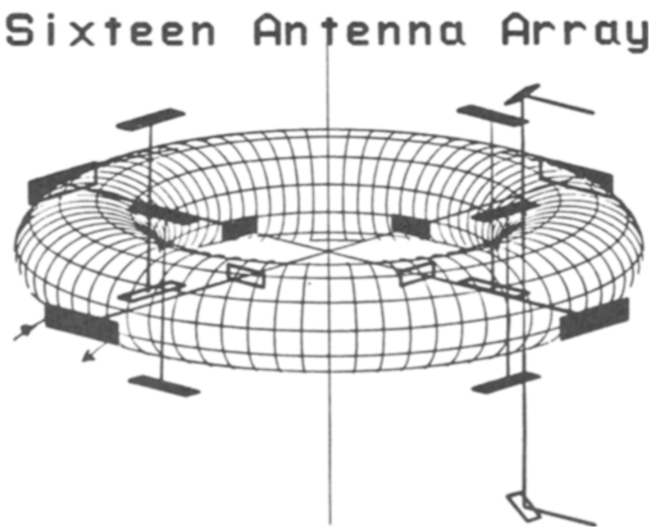

Figure 10.